THE PUBLISHING HOUSE
OF THE ROMANIAN ACADEMY

PROCEEDINGS OF THE ROMANIAN ACADEMY, Series A,
Volume 15, Number 4/2014, pp. 338–345

NEAR-FIELD AND EXTINCTION SPECTRA OF ROD-SHAPED NANOANTENNA DIMERS

Titus SANDU

National Institute for Research and Development in Microtechnologies (IMT),
126A Erou Iancu Nicolae Street, Bucharest, RO-077190, Romania
E-mail: titus.sandu@imt.ro

Plasmonic properties of rod-shaped nanoantenna dimers in a touching configuration are studied with an electrostatic method. First, a scaling law of rod nanoantennas is given in the electrostatic approximation. Furthermore, we have found that the dimer plasmon resonance corresponding to the dipolar mode of a single antenna is only slightly shifted, while a new resonance emerges in infrared. This new resonance moves deeper to larger wavelengths as the dimer junction becomes tighter. The maximum of the field enhancement is at the ends of a single nanoantenna. The dimer still has the same field enhancement at its ends, but a much larger enhancement is obtained in the dimer gap. The field enhancement of the dimer outperforms also the enhancement of nanoantennas of the same length.

Key words: localized surface plasmon resonance, Laplace equation, boundary integral equation, polarizability, nanoantenna.

1. INTRODUCTION

Free electrons in noble metals exhibit collective excitations in both propagating and localized forms at the interface with dielectrics. If the separating surface is unbounded there are running waves as surface plasmon polariton (SPP) modes whilst for metallic nanoparticles one encounters localized surface plasmon resonance (LSPR) modes. These collective electron oscillations show interesting properties with various applications in sensing, either as refractive index sensing [1] or as surface enhanced Raman spectroscopy (SERS) [2], metamaterials [3], waveguiding [4], or enhanced coupling to active semiconductor components like photovoltaic cells [5], and SPASERs, i.e., quantum amplifiers of surface plasmons by stimulated emission of radiation [6].

Two main properties are mostly used in all these applications: large absorption/scattering cross-sections and efficient confinement of electromagnetic fields below the diffraction limit. The confinement of the electromagnetic field leads to large enhancement of the electric field that is widely used in surface-enhanced spectroscopies, such as surface enhanced infrared spectroscopy (SEIRS) [7] or SERS [2]. The sensing in such surface-enhanced spectroscopies occurs at specific spots also called hotspots with the largest field enhancement [2, 7]. Large near-field enhancements are obtained around sharp tips [8] or in the intra-space of aggregates made of metallic nanoparticles such as dimers [9]. The near-field enhancement becomes stronger as the nanoparticles of the dimer get closer [10]. Moreover, in the limiting case of touching a new plasmon resonance mode is created [10, 11] with huge near field enhancement. The new mode is called the charge transfer mode and is situated in the infrared (IR) band of optical spectrum [11], being appropriate for SEIRS applications.

The interaction of metallic nanoparticle with light can be successfully described by classical methods that basically integrate the Maxwell equations. Fully quantum mechanical calculations show that the classical methods are quite accurate most of the time [12]. Thus, a number of classical numerical methods like the discrete dipole approximation [13] used initially for modeling light scattering by stellar dust, the boundary element method [14], or finite-difference time domain and multipole expansion methods [15] have been used to describe plasmon resonances in metallic nanoparticles. Whenever the size of the nanoparticle is

much smaller than the light wavelength the electrostatic approximation becomes valid and the electric and magnetic fields decouple in the Maxwell equations. Thus, the description of plasmon resonances resides in the resolution of Laplace equation for the electric field with a more transparent boundary integral equation (BIE) method [16]. In BIE the plasmon modes are electrostatic resonances which are represented by surface charge modes. The BIE method permits the separation of the optical response in a geometrical part and a dielectric or material-based part [11, 16], which can be successfully applied in the design of plasmonic structures [17, 18].

The success of Maxwell equations in describing optical response of metallic nanoparticles ensured the application of other concepts used in radiofrequency and microwave spectrum. One of such concepts is that of optical antenna or nanoantenna [19]. The major difference between the radio and optical antennas is the penetration depth, which is negligible in radiofrequency but finite at optical frequencies [20]. It leads, for instance, to a different wavelength scaling for the optical counterpart of a λ/2 radio antenna [19, 20]. Properties like antenna impedance, efficiency, directivity or gain are now used in optical antennas for antenna-enhanced fluorescence and antenna-enhanced Raman scattering in addition to the field enhancement due to the localized surface plasmon resonances.

One of the simplest prototypes of optical antenna is the rod-like nanoantenna. It has a good directivity [21] and it is easy to optimize its size and dimensions [22]. In recent works there were assessed both the far-field [23] as well as the near-field [24] plasmonic properties of a single nanorod antenna with respect to electrostatic approximation. The conclusion was that for nanorods with the length bellow 100 nm the plasmonic properties calculated by integrating the Maxwell equations were in good agreement with the results obtained by the electrostatic version of the BIE method. The nanorod dimers made of rod-like nanoantennas combine the advantages of dimer arrangement with the properties of nanoantennas. Also, in order to have plasmon resonances in infrared for SEIRS applications one needs micrometer long nanoantennas [25]. In the present work we study the electrostatic scaling law of rod-shaped nanoantennas as well as the near-field and extinction spectra of nanorod dimers. We found that, compared with single rod nanoantennas, the dimers exhibit a new resonance mode in the infrared and a much larger near-field enhancement. The plasmon modes in dimers can be explained in terms of mode hybridization with large charge accumulation and variation that lead the large field enhancement [11]. Our calculations also show that nanorod dimers have larger field enhancement than a sole nanoantenna of the same length.

The paper has the following structure. In section 2 we describe the BIE method that allows the electrostatic analysis of plasmon resonances. Then in the next section we present the fully numerical results. The conclusions are summarized in the last section.

2. THEORETICAL PRELIMINARIES

In the quasi-static limit the resolution of Maxwell equations reduces to Laplace equation for dielectrically heterogeneous systems. Let us consider an arbitrarily shaped nanoparticle that determines a domain Ω of volume V and is bounded by the surface Σ. The following operators defined on Σ can be used to solve the Laplace equation with various boundary conditions:

$$\hat{M}[u] = \frac{1}{4\pi} \int\limits_{\boldsymbol{x},\boldsymbol{y}\in\Sigma} \frac{u(\boldsymbol{y})\boldsymbol{n}(\boldsymbol{x})\cdot(\boldsymbol{x}-\boldsymbol{y})}{|\boldsymbol{x}-\boldsymbol{y}|^3} \mathrm{d}\Sigma(\boldsymbol{y}) \tag{1}$$

its adjoint $\hat{M}^{\dagger}$

$$\hat{M}^{\dagger}[v] = \frac{1}{4\pi} \int\limits_{\boldsymbol{x},\boldsymbol{y}\in\Sigma} \frac{v(\boldsymbol{y})\boldsymbol{n}(\boldsymbol{y})\cdot(\boldsymbol{x}-\boldsymbol{y})}{|\boldsymbol{x}-\boldsymbol{y}|^3} \mathrm{d}\Sigma(\boldsymbol{y}) \tag{2}$$

and the symmetric and non-negative Coulomb operator

$$\hat{S}[u] = \frac{1}{4\pi} \int\limits_{\boldsymbol{x},\boldsymbol{y}\in\Sigma} \frac{u(\boldsymbol{y})}{|\boldsymbol{x}-\boldsymbol{y}|} \mathrm{d}\Sigma(\boldsymbol{y}) . \tag{3}$$

In Eqs. (1–3) $\boldsymbol{n}$ is the normal vector to Σ. The operator $\hat{M}$ can be made symmetric and even self-adjoint via the Plemelj's symmetrization principle $\hat{M}^{\dagger}\hat{S}=\hat{S}\hat{M}$ [11]. In this way the operator $\hat{M}$ is symmetric with respect to the inner product defined by $\langle v|u\rangle_S=\langle v|\hat{S}[u]\rangle$, where $\langle\ |\ \rangle$ defines the standard inner product on $L^2(\Sigma)$ and $\langle\ |\ \rangle_S$ is the inner product determined by $\hat{S}$. We recall here that the inner product of two functions $u_1(\boldsymbol{x})$ and $u_2(\boldsymbol{x})$ belonging to $L^2(\Sigma)$ is defined as $\langle u_1|u_2\rangle=\int\limits_{\boldsymbol{x}\in\Sigma} u_1^*(\boldsymbol{x})\ u_2(\boldsymbol{x})\mathrm{d}\Sigma(\boldsymbol{x})$, where the star sign * signifies the complex conjugate of a complex number. The operators $\hat{M}$ and $\hat{M}^{\dagger}$ have the same spectrum bounded from below by –1/2 and from above by 1/2 [11, 26]. The eigenfunctions u_i of $\hat{M}$ are related to the eigenfunctions by v_i of $\hat{M}^{\dagger}$ by $v_i=\hat{S}[u_i]$, which makes them bi-orthogonal, i.e. $\langle v_j|u_i\rangle=\delta_{ij}$. In physical terms $\hat{M}[u]$ signifies to the normal component of the electric field that is generated by the surface charge density *u*. On the other hand v_i is the electric potential generated on surface Σ by the dipole distribution u_i. The largest eigenvalue is always 1/2 which does not have any plasmonic significance but its eigenmode is related to the charging and electrostatic capacitance of the metallic object [27].

If we consider that the the complex permittivity of the metallic nanoparticle is ϵ_1 (usually a Drude-like form $\epsilon_1(\omega)=\varepsilon_m-\omega_p^2/\left(\omega(\omega+\mathrm{i}\gamma)\right)$ and of the embedding medium is ϵ_0 (usually a real constant) then the induced surface charge density u_{E_0} due to the impinging uniform and harmonic electric field $\boldsymbol{E}_0\boldsymbol{e}^{\boldsymbol{i}\omega t}$ is [11,16,26]

$$u_{E_0}=\sum_k\frac{\langle v_k\,|\,\boldsymbol{n}\cdot\boldsymbol{E}_0\rangle}{\frac{1}{2\lambda}-\chi_k}u_k. \tag{4}$$

Here $\lambda=(\epsilon_1-\epsilon_0)/(\epsilon_1+\epsilon_0)$, while χ_k are the eigenvalue of M and $M^{\dagger}$, and $\boldsymbol{n}\cdot\boldsymbol{E}_0$ is the dot product of two vectors in 3D. The knowledge of the induced charge density allows us to calculate the far-field optical response as well as the near-field behavior. In the far-field it survives only the dipolar component which is encompassed in specific polarizability α [16, 26]

$$\alpha=\sum_k\frac{1}{V}\frac{\langle\boldsymbol{x}\cdot\boldsymbol{N}|u_k\rangle\langle v_k\,|\,\boldsymbol{n}\cdot\boldsymbol{E}_0\rangle}{\frac{1}{2\lambda}-\chi_k}. \tag{5}$$

The specific polarizability is simply the dipole moment generated by u_{E_0} divided by the volume *V* of the nanoparticle. The imaginary part of α is proportional to the extinction cross-section $C_{ext}=\frac{2\pi}{\lambda}\mathrm{Im}(\alpha V)$ [28]. From Eqs. (4) and (5) we can state that the charge density u_{E_0} and the specific polarizability α are sums over all eigenmodes that represent the plasmon (electrostatic) resonances. The same is true for near-field properties. A near-field characteristic is the field enhancement at the nanoparticle surface. It turns out that the expression for near-field enhancement is quite similar to the far-field. Thus the components of near-field enhancement normal and tangent to Σ are, respectively [11]

$$E_n(\xi_1,\xi_2)=\sum_k\frac{\langle v_k\,|\,\boldsymbol{n}\cdot\boldsymbol{E}_0\rangle(\chi_k+1/2)}{\frac{1}{2\lambda}-\chi_k}u_k(\xi_1,\xi_2), \tag{6}$$

and

$$\boldsymbol{E}_t(\xi_1,\xi_2)=-\sum_{\substack{k,\\ i=1,2}}\frac{\langle v_k\,|\,\boldsymbol{n}\cdot\boldsymbol{E}_0\rangle}{\frac{1}{2\lambda}-\chi_k}\frac{1}{h_{\xi_i}}\frac{\partial v_k(\xi_1,\xi_2)}{\partial\xi_i}\boldsymbol{t}_{\xi_i}, \tag{7}$$

where ξ_1 and ξ_2 are the parameters defining Σ, whose tangent vectors are $\boldsymbol{t}_{\xi_1}$ and $\boldsymbol{t}_{\xi_2}$. Also $\boldsymbol{h}_{\xi_1}$ and $\boldsymbol{h}_{\xi_2}$ are the Lamé coefficients associated with Σ. For a Drude model of metal the factor $\left(\frac{1}{2\lambda}-\chi_k\right)^{-1}$ has an explicit form [11, 16]

$$\frac{1}{\frac{1}{2\lambda}-\chi_k}=A-\frac{1}{1/2-\chi_k}\frac{\varepsilon_o}{\varepsilon_{eff\_k}}\frac{\tilde{\omega}_{pk}^2}{\omega\left(\omega+i\gamma\right)-\tilde{\omega}_{pk}^2}, \tag{8}$$

where ε_o is dielectric permittivity of the embedding medium, assumed to be constant and real, A is a determined constant and

$$\tilde{\omega}_{pk}=\omega_p\sqrt{\left(1/2-\chi_k\right)/\varepsilon_{eff\_k}} \tag{9}$$

is the localized plasmon resonance frequency. Also, $\varepsilon_{eff\_k}=\left(1/2+\chi_k\right)\varepsilon_d+\left(1/2-\chi_k\right)\varepsilon_m$ is an effective permittivity. We note here that the term $1/2-\chi_k$ is also called depolarization factor [26, 28]. Equations (5–7) are numerically implemented by invoking a spectral method that calculates explicitly the eigenvalues and eigenfunctions of M and $M^{\dagger}$ [26, 27].

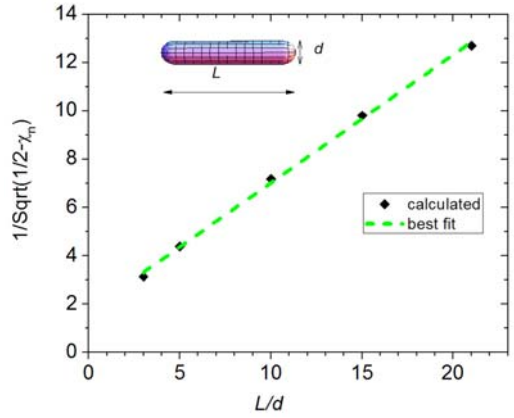

Fig. 1 – The scaling law of nanoantenna in the electrostatic limit. The symbols represent the numerical results, while the green dashed line is the best linear fit to numerical calculations. The inset shows the rod antenna and its dimensions.

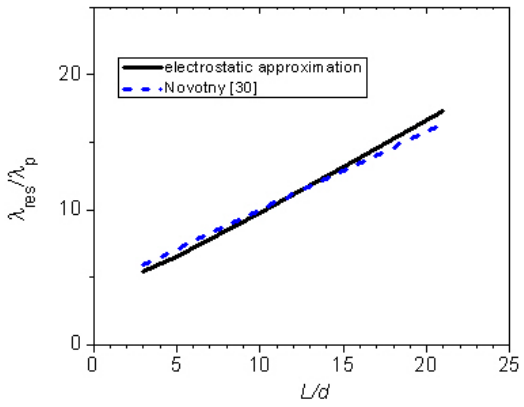

Fig. 2 – The ratio of plasmon resonance wavelength and plasma wavelength of the bulk metal with the electrostatic scaling (black solid line) and with the scaling given by Novotny [30].

3. RESULTS

In the following we will consider that our rod-shaped nanoantennas have spherical caps, are made of gold, and are immersed in water. The gold parameters of the Drude model $\epsilon\left(\omega\right)=\varepsilon_m-\omega_p^2/\left(\omega\left(\omega+i\gamma\right)\right)$ are: 9 eV for ω_p, 0.1 eV for γ, and $\varepsilon_m=10.2$. These parameters are tuned such that one can obtain a plasmon resonance at 520 nm for a nanosphere. The electrostatic approximation is a scale invariant theory; hence we characterize our nanoantennas just by their aspect ratio (the ratio between their length and their diameter). For radio antennas their lengths are directly related to wavelength of the radiation like in the case of half-wave dipole antenna that is made of a thin metallic rod [29]. Thus, for that antenna its length is half of the wavelength of incoming radiation. At optical frequency, however, due to the skin depth, which is comparable with the thickness of nanoantenna, another scaling law holds. Recently it was shown that there is a linear relationship between the light wavelength at which the plasmon resonance occurs and the length of nanoantenna [30]

$$\lambda_{res} = a + bL\,, \tag{10}$$

where λ_{res} is the wavelength resonance, L is the nanorod length, and a and b are some constants. Because of the scale invariance, in the electrostatic limit the length L must be replaced by the aspect ratio L/d. Thus considering Eq. (9), the linear scaling given by Eq. (10) takes the form of depolarization factor scaling in the electrostatic approximation

$$\frac{1}{\sqrt{1/2 - \chi_k}} = n + m\frac{L}{d}\,. \tag{11}$$

The numerical verification is presented in Fig. 1. The linear fit gives n = 1.71487 and m = 0.53037. In Ref. [30] Eq. (10) was deduced by presuming long rods, but the linear fit illustrated in Fig. 1 shows that Eq. (11) holds even for small aspect ratios. Combining Eqs. (9) and (11) we determined the coefficients a and b of Eq. (10) in the electrostatic limit and from Eq. (14) of Ref. [30] we determined a and b given by the Novotny paper. Their comparison is given in Fig. 2 showing a quite good agreement over a large aspect ratio range.

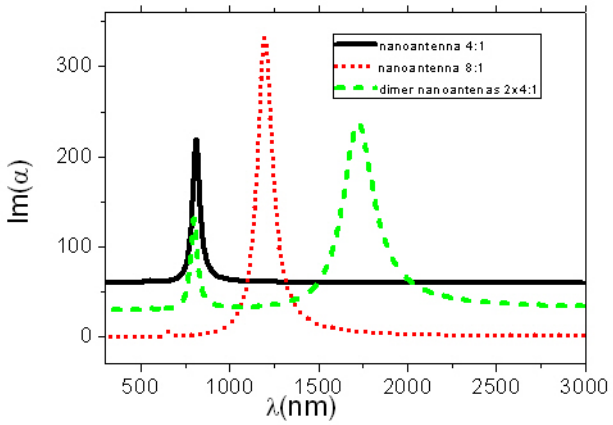

Fig. 3 – The imaginary part of specific polarizability (a dimensionless quantity) for the 4:1 antenna (black solid line), dimer 4:1 (green dashed line), and 8:1 antenna (red dotted line). The plots are up-shifted for a better visualization.

As we have discussed before, the plasmon response of metallic nano-objects with dimensions below 100 nm can be successfully described within the electrostatic approximation [24]. We choose a nanoantenna with an aspect ratio of 4:1 (see the inset of Fig. 4), a dimer made of two antennas with the same aspect ratio of 4:1 (see the inset of fig. 5), and for comparison a nanoantenna with an aspect ratio of 8:1 (hence this nanoantena has the same length as the dimer). The cross-section of the dimer gap is 20% of the full cross-section. This type of geometrical setup is possible with the new nanofabrication techniques that can craft junctions below 10 nm in cross-section [31, 32]. The optical extinction is determined by the imaginary part of the specific polarizability (Fig. 3). The main resonance mode (at about 750 nm) for a simple nanoantenna (4:1) is the dipole mode, which almost coincides with its corresponding hybrid mode in the dimer. The dimer mode is a hybridization of dipole modes in the constituent rod antennas [11]. Due to a sum rule [26] the dipole resonance in the dimer has smaller weight since an additional plasmon resonance show up in the infrared [11]. This new resonance is usually called the charge transfer mode since it does not appear in non-connected dimers [14]. Its corresponding surface charge mode is a hybrid mode of the net-charging modes on each rod antenna, thus it is positive on one antenna and negative on the other one, with huge charge accumulation in the junction. The net-charging mode, however, is not an active plasmon mode by itself, but its hybrid can be active in dimers [11, 14]. On the other hand the longer nanoantenna (with an 8:1 aspect ratio) has its dipole resonance red-shifted in infrared. We note here that the impinging field is parallel to antenna axis, the perpendicular configuration exhibiting a weaker plasmon resonance.

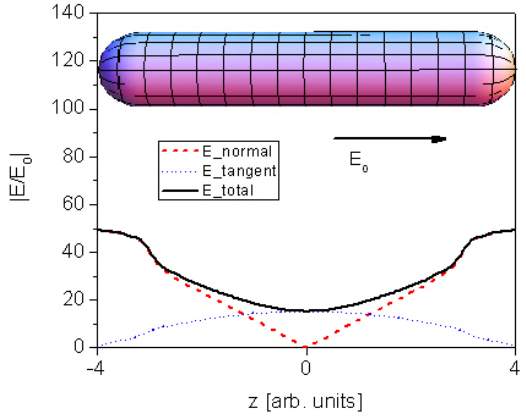

Fig. 4 – The field enhancement for the dipole resonance of a 4:1 nanoantena. The black solid line is the total enhancement, which is decomposed in a tangent part (blue dotted line) and normal part (red dashed line).

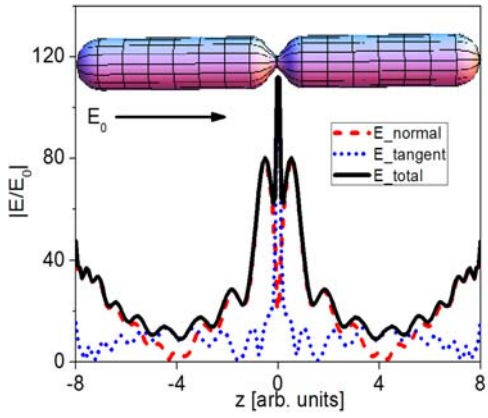

Fig. 5 – The field enhancement for the dipole resonance of a dimer nanoantena. The black solid line is the total enhancement, which is decomposed in a tangent part (blue dotted line) and normal part (red dashed line).

In Fig. 4 we show the field enhancement for the main (dipole) resonance of a 4:1 nanoantenna. The impinging field is parallel to antenna axis, thus the response is also axially symmetric and only the longitudinal dependence is presented. The maximum field enhancement reaches a value of 50 at the ends of the antenna. On the other hand, the dimer presented in Fig. 5 has the same enhancement at its ends, but in the gap junction the enhancement surpasses 100. This large enhancement in the gap is also due to charge accumulation, such that narrower junctions lead to even stronger enhancements [11]. The analysis of the field component shows us that at the ends the normal component is dominant but in the junction region there is a play between tangent and normal components such that a strong maximum occurs at the middle of the junction. The field enhancement for an 8:1 nanoantenna (Fig. 6) has a similar shape as the 4:1 nanoantenna, but the maximum enhancement is about 70 in comparison to an enhancement of 50 for a 4:1 antenna.

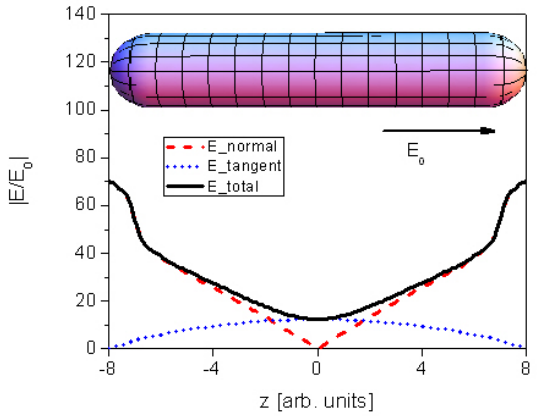

Fig. 6 – The field enhancement for the dipole resonance of an 8:1 nanoantena. The black solid line is the total enhancement, which is decomposed in a tangent part (blue dotted line) and normal part (red dashed line).

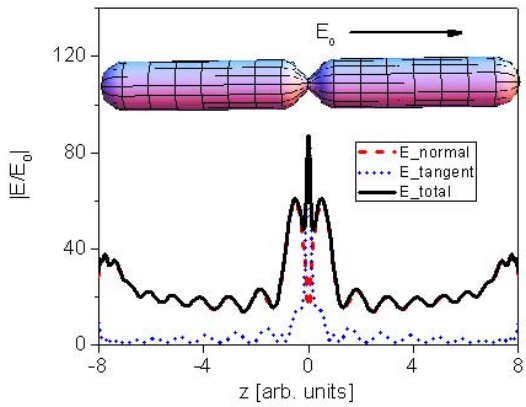

Fig. 7 – The field enhancement for the charge transfer mode resonance of a dimer nanoantena. The black solid line is the total enhancement, which is decomposed in a tangent part (blue dotted line) and normal part (red dashed line).

Strong field enhancement is also obtained for the charge transfer mode. In Fig. 7 we plotted the field enhancement for the charge transfer mode. The ends of the dimer have an enhancement of almost 40 but the field at the junction attains a value above 80. Thus, even tough the charge transfer mode has a smaller enhancement than the dipole originating mode, the enhancement is bigger than that of 8:1 nanoantenna.

The validity of the electrostatic method is limited to nano-objects with dimensions below 100. For bigger nano-objects retardation and radiation damping begin to play a significant role [28]. Thus, by retardation the resonances move to infrared and higher multipole resonances become stronger and observable. Higher multipole resonances are also present in the electrostatic approximation but their

presence is manifested by quite small humps. The near-field is degraded also by radiation broadening, which can be viewed as the enlargement of broadening factor γ in Eq. (8) [28].

4. CONCLUSIONS

In summary, we have analyzed the plasmon properties of nanorod dimers and compared them with the properties of simple nanorod antennas. First, we have elaborated a scaling law that relates the main (dipolar) plasmon wavelength resonance to the aspect ratio of the rod-shaped nanoantenna in the electrostatic limit. In the case of the dimer the corresponding plasmon resonance is only slightly shifted. In contrast to a single nanorod antenna the dimer has a new resonance in infrared. The new resonance is more red-shifted as the junction of the dimer becomes narrower. As a general trend, the near-field enhancement is maximal at the ends of the antenna. The dimer preserves the field enhancement at its ends but a much larger near-field enhancement is obtained in its gap, with larger enhancements for tighter junctions. Finally, the field enhancement of the dimer is even larger than that of a rod nanoantenna of the same length.

ACKNOWLEDGEMENT

This work was supported by a grant of the Romanian National Authority for Scientific Research, CNCS—UEFISCDI, Project Number PNII-ID-PCCE-2011-2-0069.

REFERENCES

1. J.N. ANKER, W. PAIGE HALL, O. LYANDRES, N.C. SHAH, J. ZHAO, R.P. Van DUYNE, *Biosensing with plasmonic nanosensors*, Nat. Mater., **7**, pp. 442–453, 2008.
2. S. NIE, S.R. EMORY, *Probing Single Molecules and Single Nanoparticles by Surface-Enhanced Raman Scattering*, Science, **275**, pp. 1102–1106, 1997.
3. K. LODEWIJKS, N. VERELLEN, W. VAN ROY, G. BORGHS, P.VAN DORPE, *Self-assembled hexagonal double fishnets as negative index materials*, Appl. Phys. Lett., **98**, 091101, 2011.
4. S. LAL, S. LINK, N.J. HALAS, *Nano-optics from sensing to waveguiding*, Nature Photonics, **1**, pp. 641–648, 2007.
5. H.A. ATWATER, A. POLMAN, *Plasmonics for improved photovoltaic devices*, Nat. Mater., **9**, pp. 205–213, 2010.
6. N.I. ZHELUDEV, S.L. PROSVIRNIN, N. PAPASIMAKIS, V.A. FEDOTOV, *Lasing spaser*, Nat. Photon., **2**, pp. 351–354, 2008.
7. L. FEI, D.W. BRANDL, Y.A. URZHUMOV, H. WANG, J. KUNDU, N.J. HALAS, J. AIZPURUA, P. NORDLANDER, *Metallic nanoparticle arrays: a common substrate for both surfaceenhanced Raman scattering and surface-enhanced infrared absorption*, ACS Nano, **2,** pp. 707–718, 2008.
8. L. NOVOTNY, R.X. BIAN, X.S. XIE, *Theory of Nanometric Optical Tweezers*, Phys. Rev. Lett., **79**, pp. 645–648, 1997.
9. T. ATAY, J.H. SONGA, A.V. NURMIKKO, *Strongly interacting plasmon nanoparticle pairs: from dipole-dipole interaction to conductively coupled regime*, Nano Lett., **4**, pp. 1627–1633, 2004.
10. F.J. GARCÍA DE ABAJO, A. HOWIE, *Retarded field calculation of electron energy loss in inhomogeneous dielectrics*, Phys. Rev. B, **65**, 115418, 2002.
11. T. SANDU*, Eigenmode Decomposition of the Near-Field Enhancement in Localized Surface Plasmon Resonances of Metallic Nanoparticles*, Plasmonics, **8**, pp. 391–402, 2013.
12. J. ZULOAGA, E. PRODAN, P. NORDLANDER, *Quantum description of the plasmon resonances of a nanoparticle dimmer*, Nano Lett., **9**, pp. 887–891, 2009.
13. L. GUNNARSON, T. RINDZEVICIUS, J. PRIKULIS, B. KASEMO, M. KÄLL, S. ZOU, G.C. SCHATZ, *Confined plasmons in nanofabricated single silver particle pairs: experimental observations of strong interparticle interactions*, J. Phys. Chem. B, **109**, pp. 1079–1087, 2005.
14. I. ROMERO, J. AIZPURUA, G.W. BRYANT, F.J. GARCÍA DE ABAJO, *Plasmons in nearly touching metallic nanoparticles: singular response in the limit of touching dimers*, Opt. Exp., **14**, pp. 9988–9999, 2006.
15. B. KHLEBTOV, A. MELNIKOV, V. ZHAROV, N. KHLEBTOV, *Absorption and scattering of light by a dimer of metal nanospheres: comparison of dipole and multipole approaches*, Nanotechnology, **17**, pp. 1437–1445, 2006.
16. T. SANDU, D. VRINCEANU, E. GHEORGHIU, *Surface Plasmon Resonances of Clustered Nanoparticles*, Plasmonics, **6**, pp. 407–412, 2011.
17. T. SANDU, *Shape effects on localized surface plasmon resonances in metallic nanoparticles*, J. Nanopart. Res., **14**, pp. 905, 2012.
18. T.J. DAVIS, K.C. VERNON, D.E. GOMEZ, *Designing plasmonic systems using optical coupling between nanoparticles*, Phys. Rev. B, **79**, 155423, 2009.
19. L. NOVOTNY, N. VAN HULST, *Antennas for light*, Nature Phot., **5**, pp. 83–90, 2011.
20. P. BHARADWAJ, B. DEUTSCH, L. NOVOTNY, *Optical Antennas*, Adv. in Optics and Photonics, **1**, pp. 438–483, 2009.

21. A. AHMED, R. GORDON, *Directivity Enhanced Raman Spectroscopy Using Nanoantennas*, Nano Lett., **11**, pp. 1800–1803, 2011.
22. J.S. SEKHON, S.S. VERMA, *Optimal dimensions of gold nanorod for plasmonic nanosensors*, Plasmonics, **6**, pp. 163–170, 2011.
23. T.J. DAVIS, K.C. VERNON, D.E. GOMEZ, *Effect of retardation on localized surface plasmon resonances in a metallic nanorod*, Opt. Express, **17**, pp. 23655–23663, 2009.
24. T. SANDU, V. BUICULESCU, *Near-Field Enhancement of a Rod-like Nanoantenna: Electrostatic Versus Fully Retarded results,* IEEE Proceedings CAS-International Semiconductor Conference, Vol. 2, 2012, pp. 415–418.
25. R. ADATO, A.A. YANIK, J.J. AMSDEN, D.L. KAPLAN, F.G. OMONETTO, M.K. HONG, S. ERRAMILLI, H. ALTUG, *Ultra-sensitive vibrational spectroscopy of protein monolayers with plasmonic nanoantenna arrays*, Proc. Natl. Acad. Sci., **106**, pp. 19227–19232, 2009.
26. T. SANDU, D. VRINCEANU, E. GHEORGHIU, *Linear dielectric response of clustered living cells*, Phys. Rev. E, **81**, 021913, 2010.
27. T. SANDU, G. BOLDEIU, V. MOAGAR-POLADIAN, *Applications of electrostatic capacitance and charging*, J. Appl. Phys., **114**, 224904, 2013.
28. S.A. MAIER, *Plasmonics: fundamentals and applications*, Springer, New York, 2007.
29. T. MILLIGAN, *Modern Antenna Design*, McGraw-Hill, New York, 1985.
30. L. NOVOTNY, *Effective Wavelength Scaling for Optical Antennas*, Phys. Rev. Lett., **98**, 266802, 2007.
31. M. SCHNELL, A. GARCIA-ETXARRI, A.J. HUBER, K. CROZIER, J. AIZPURUA, R. HILLEBRAND, *Controlling the near-field oscillations of loaded plasmonic nanoantennas*, Nature Photon., **3**, pp. 287–291, 2009.
32. K. UENO, H. MISAWA, *Fabrication of Nanoengineered Metallic Structures and Their Application to Nonlinear Photochemical Reactions*, Bull. Chem. Soc. Jpn., **85**, pp. 843–853, 2012.

Received May 6, 2014